Plant Ecology and Evolution 157 (2): 113–124, 2024
https://doi.org/10.5091/plecevo.115801

RESEARCH ARTICLE

The genus *Orthoseira* (Orthoseiraceae, Bacillariophyta) in Papua New Guinea with the description of two new species

Natalia Kochman-Kędziora[1], Bart Van de Vijver[2,3]

1 Department of Ecology and Environmental Protection, University of Rzeszów, Rzeszów, Poland
2 Meise Botanic Garden Meise, Research Department, Meise, Belgium
3 University of Antwerp, Department of Biology – ECOSPHERE, Wilrijk, Belgium

Corresponding author: Bart Van de Vijver (bart.vandevijver@plantentuinmeise.be)

Academic editor: Christine Cocquyt ♦ **Received** 15 November 2023 ♦ **Accepted** 24 January 2024 ♦ **Published** 13 March 2024

Abstract

Background and aims – The genus *Orthoseira* is generally known to be typically aerophilous. Despite the worldwide occurrence of the genus, most of the *Orthoseira* species seem to have a rather restricted biogeographic distribution, often being part of an endemic diatom flora. During a survey of the aerophilic diatom flora in Papua New Guinea (Karkar Island, Boisa Island), four morphologically distinct *Orthoseira* taxa have been observed.
Material and methods – The morphology of four *Orthoseira* species was investigated in detail using light microscopy (LM) and scanning electron microscopy (SEM).
Key results – The morphology of all four species is discussed and compared to known species worldwide. The main differences between the species include: the presence and shape of linking structures, the number of rows of perforations on the copulae, presence/absence of internal caverns and the external structure of the carinoportulae. Two species, with a unique set of features, are described as new to science: *Orthoseira iserentantii* sp. nov. and *Orthoseira papuensis* sp. nov.
Conclusions – The observation of four *Orthoseira* species, including two species new to science, confirms that the diversity of the genus *Orthoseira* is underestimated.

Keywords

morphology, new species, *Orthoseira*, Papua New Guinea

INTRODUCTION

The diatom genus *Orthoseira* Thwaites (Orthoseiraceae, Bacillariophyta) was originally described in 1848 based on *Melosira americana* Kütz. (Kützing 1844). In its current concept, the genus encompasses a group of mostly aerophilous non-pennate diatoms with radial symmetry, a flat valve face and several distinct central tube-like pores, called carinoportulae (Crawford 1981). Following the latest molecular studies, revealing a close phylogenetic relationship with the 'multipolar' diatoms, representatives of the genus *Orthoseira* are now placed in the order Orthoseirales, class Mediophyceae (Gargas et al. 2018). Apart from the shared feature of the carinoportulae, members of the genus *Orthoseira* are characterized by quite some variability in their morphological features (Houk 1993; Houk et al. 2017). Moreover, a discussion of the taxonomic history of the genus *Orthoseira* indicated the unclear taxonomic identity of the genus (Danz et al. 2022) since the designated typus generis, *M. americana*, entirely lacks the presence of carinoportulae, a feature not even included in the genus description. Danz et al. (2022) recommended that the name *Orthoseira* should be restricted only for *M. americana*. A revision of all known *Orthoseira* species is currently being undertaken (Kociolek et al. unpubl. res.), taking also into account three

Plant Ecology and Evolution is published by Meise Botanic Garden and Royal Botanical Society of Belgium.

genera that were described by Ehrenberg in 1848, several months after the description of the genus *Orthoseira* by Thwaites (1848) (Ehrenberg 1848), these three genera all possessing carinoportulae (i.e. *Liparogyra* Ehrenb., *Porocyclia* Ehrenb., and *Stephanosira* Ehrenb.). Together with the revision of the already described *Orthoseira* species, the analysis of unidentified populations of possible *Orthoseira* species worldwide is another crucial step towards a better understanding of this group of species. This has led to a steep increase in the number of *Orthoseira* species during the past years. According to AlgaeBase, there are currently 34 accepted names (species and formae included) in *Orthoseira* (Guiry and Guiry 2023). The past years, species have been described from the sub-Antarctic region, Argentina, the United States, Greenland, Switzerland, South East Asia, Easter Island, and China (Van de Vijver and Kopalová 2008; Lowe et al. 2013; Guerrero et al. 2018; Kociolek et al. 2021; Danz and Kociolek 2022; Rybak et al. 2022; Goeyers et al. 2023; Peszek et al. 2023).

The genus *Orthoseira* is generally known to be typically aerophilous, usually observed in samples collected from wet rocks, the spray zone of waterfalls, moss carpets on tree trunks, lava caves, and soils (Round et al. 1990; Lowe et al. 2013; Houk et al. 2017). The genus does not seem to be restricted to a particular climate zone as species of *Orthoseira* have been reported from the tropics to the polar regions (Van de Vijver et al. 2004; Van de Vijver and Kopalová 2008; Lowe et al. 2013; Houk et al. 2017; Danz and Kociolek 2022; Goeyers et al. 2023). Despite this worldwide genus distribution, most of the *Orthoseira* species seem to have a rather restricted biogeographic distribution (Van de Vijver and Kopalová 2008; Lowe et al. 2013), even being part of an endemic diatom flora (Kociolek et al. 2021; Danz and Kociolek 2022; Rybak et al. 2022). On the other hand, there are still *Orthoseira* species that are often considered cosmopolitan, such as *O. roeseana* (Rabenh.) Pfitzer, described originally as *Melosira roeseana* (Rabenhorst 1853), and transferred to the genus *Orthoseira* in 1871 (Pfitzer 1871). One of the reasons of this presumable cosmopolitan occurrence is the force-fitting of local populations into the name *O. roeseana* as the morphology of this species was poorly known, and only recently studied in detail based on the analysis of its type material (Kochman-Kędziora et al. 2023).

As a result, the name *O. roeseana* is not only reported from all over the world, the morphology of *O. roeseana* has also been broadening during all these decades. The recent analysis of the type material of both *Orthoseira* (*Melosira*) *roeseana* and *O. spinosa* W.Smith (Smith 1855) proved that most *O. roeseana* populations in fact represent independent, often undescribed species (Kochman-Kędziora et al. 2023), underestimating the diversity of the genus *Orthoseira*, as confirmed by the recent description of for instance *O. tatrica* Houk, Klee & H.Tanaka (Houk et al. 2017), *O. groenlandica* Goeyers, Kochman-Kędziora & Van de Vijver (Goeyers et al. 2023), and *O. helvetica* Peszek, C.T.Robinson, Rybak & Kawecka (Peszek et al. 2023), all showing some similarity with *O. roeseana*.

During a survey of the aerophilic diatom flora in Papua New Guinea (Karkar Island, Boisa Island), four morphologically distinct *Orthoseira* taxa have been observed. Two taxa could be identified as *O. hawaiiensis* Danz & Kociolek (Danz and Kociolek 2022) and *O. tropica* (Krasske) Metzeltin & Lange-Bert. (Metzeltin and Lange-Bertalot 2007), whereas the two other taxa could not be identified using the currently available literature. Following light (LM) and scanning electron (SEM) microscopy observations, both unknown taxa are described as new species: *Orthoseira iserentantii* sp. nov. and *Orthoseira papuensis* sp. nov. Their morphology is illustrated and discussed in comparison with all known *Orthoseira* species worldwide.

MATERIAL AND METHODS

During a survey of the aerophilic diatom flora in 1987 and 1989 in Papua New Guinea (Mont Wilhelm, Karkar Island, Boisa Island), more than 100 samples were collected from mosses and liverworts on fairly dry to humid, aerial substrates such as tree trunks and roots of bushes and trees. A preliminary survey of the samples resulted in a selection of four samples containing large populations of *Orthoseira* taxa:

- sample 17 (Mont Wilhelm, Papua New Guinea, coll. date 9 Apr. 1987, leg. Martine Fagnant, no GPS data, elev. ca 3500 m a.s.l.): Heathland forest on the west bank of Lake Piunde; sample take by squeezing the water out of Hypnaceae and *Plagiochila* mosses on the trunks of some Ericaceae species.
- sample 110 (Karkar Island, Village of Mom, Papua New Guinea, coll. date 17 Dec. 1989, leg. Robert Iserentant, 145°55’00”S, 4°37’00”E, elev. 300 m a.s.l.): expression of very wet mosses growing on tree trunks in a plantation.
- sample 156 (Boisa Island, Papua New Guinea, coll. date 30 Dec. 1989, leg. Robert Iserentant, 144°57’30”S, 4°00’00”E, elev. 10 m a.s.l.): scrapings of slightly wet mosses growing on buttress roots of *Inocarpus*.
- sample 158 (Boisa Island, Papua New Guinea, coll. date 30 Dec. 1989, leg. Robert Iserentant, 144°57’30”S, 4°00’00”E, elev. 20 m a.s.l.): scrapings of more or less dry mosses growing on buttress roots of *Artocarpus*.

A subsample of each of the selected materials was prepared for LM and SEM observations following the method described in van der Werff (1955). Small volumes of each subsample were cleaned by adding 37% H_2O_2 and subsequently heating to 80°C for about 1–2 h, after which the reaction was completed by adding saturated $KMnO_4$. Following digestion and centrifugation (three times 10 minutes at 4500× rpm), the cleaned diatom material was diluted with distilled water to avoid excessive concentrations of diatom valves on a slide and mounted in Naphrax®. Slides were analysed using an Olympus BX53 microscope at ×1000 magnification (UPLanFL N 100× objective, N.A. 1.30), equipped with Differential Interference Contrast (Nomarski) optics and the Olympus UC30 Imaging System. For each taxon, the number of specimens, measured at random on the type slide, is indicated (n = X).

For SEM, parts of the oxidized suspensions were filtered through a 5-µm Isopore™ polycarbonate membrane filter (Merck Millipore). Filters were air-dried and pieces were subsequently affixed to aluminium stubs. The latter were sputter-coated with a platinum layer of at least 15 nm and studied using a JEOL-JSM-7100F field emission scanning electron microscope operated at 2 kV and 4 mm working distance (Meise Botanic Garden, Belgium). Slides, samples and stubs analysed in this study are stored at the BR collection (Meise Botanic Garden, Belgium). Plates were prepared using Photoshop CS5.

Terminology used for the description of the various structures of the siliceous cell wall is based on Ross et al. (1979, areola structure), Crawford (1981, *Orthoseira* genus features), and Houk et al. (2017, *Orthoseira* genus features). For the taxonomic treatment, the following papers were consulted: Van de Vijver and Kopalová (2008), Lowe et al. (2013), Houk et al. (2017), Guerrero et al. (2018), Kociolek et al. (2021), Danz and Kociolek (2022), Rybak et al. (2022), Goeyers et al. (2023), Kochman-Kędziora et al. (2023), and Peszek et al. (2023).

For typification of the new species, we chose to use the entire slide as the holotype following Art. 8.2 of the International Code for Botanical Nomenclature (Turland et al. 2018). An appropriate image is linked to the designated type by stating "Fig. X illustrates the type", ensuring that the identity of the species can be fixed.

RESULTS

The observations of the *Orthoseira* populations in the samples from Papua New Guinea allowed the separation of four different *Orthoseira* taxa. Two populations could be identified as taxa that were previously described: *Orthoseira hawaiiensis* and *O. tropica*. The two other taxa are described as new following a thorough comparison with all previously recognised species: *Orthoseira iserentantii* sp. nov. and *O. papuensis* sp. nov. The morphology of all four species is discussed and compared to known species worldwide.

Orthoseira hawaiiensis Danz & Kociolek

Fig. 1

Material used. Sample 110 (Karkar Island, Village of Mom, Papua New Guinea).

LM description. Frustules cylindrical in girdle view, usually solitary. Valves disc-shaped. Valve dimensions (n = 15): diameter 13–30 µm, mantle height 5.0–7.5 µm. Valve surface flat, sloping abruptly at the valve face/mantle junction, visible in LM as a darker circular edge. Central area small, maximum 1/4 to 1/5 of the total valve diameter, rounded. Three (very rarely 2) large, rounded carinoportulae present, number constant irrespective of the valve diameter. Valve face areolae small, arranged in radiate, uniseriate striae of variable length, 18–24 in 10 µm. Striae often branching near the valve margin. Short, irregular ridges present, scattered over the entire valve face, visible at different focal level (Fig. 1A). Presence of caverns along the edge of the mantle, visible as regular, darker areas, 5–7 per valve. Figure 1A–D.

SEM description. Cingulum composed of several broad, open, ligulate copulae, perforated with at least 5–7 parallel rows of very small pores (Fig. 1E–G). Valvocopula with thin, broad extensions, covering plate-like the valve interior (Fig. 1F, M). Mantle shallow (Fig. 1E, G), occasionally with a clear step halfway the valve mantle (Fig. 1E). Advalvar part of the mantle with regular striation pattern. Mantle striae composed of up to 10 areolae, 22–25 in 10 µm (Fig. 1E, G). Valve face flat. Central area hyaline, small. Three (rarely two, see Fig. 1E) carinoportulae visible with raised, irregularly shaped, cylindrical collar (Fig. 1H, I), occasionally obscured by a plate-like covering (Fig. 1H). Valve face entirely covered by an often network-like raised pattern of ridges (Fig. 1E, H–J). Halfway between valve edge and centre, several much denser groupings of short and longer ridges present, regularly placed in a ring around the central area (Fig. 1E, H–J). Striae uniseriate, composed of small, rimmed areolae (Fig. 1J). Short, thick acute marginal spines present at the valve face/mantle junction (Fig. 1E, G). Marginal pore fields present (Fig. 1E, G). Areolae covered in the valve interior by individual hymenate vela (Fig. 1K, L). Carinoportulae pit-like, visible as large, rounded depressions, filled with irregular siliceous outgrowths (Fig. 1K, L). Between the carinoportulae, several long slits present, arranged in a star-shaped manner (Fig. 1L). Internal caverns visible as shallow depressions on the valve face/mantle junction (Fig. 1K). Figure 1E–M.

Orthoseira tropica (Krasske) Metzeltin & Lange-Bert.

Fig. 2

Melosira roeseana var. *tropica* Krasske, 1948 (**basionym**), Svensk Botanisk Tidskrift 42: 422, fig. 1: 1–2 (Krasske 1948).

Orthoseira roeseana var. *tropica* (Krasske) Lange-Bert. & Willmann in Lange-Bertalot et al. (1996).

Material used. Sample 156 (Boisa Island, Papua New Guinea).

LM description. Frustules short, cylindrical in girdle view, connected to each other with spines forming short chains (Fig. 2F). Valves disc-shaped. Valve dimensions (n = 15): diameter 9.5–39.0 µm, mantle height 5–14 µm. Valve surface flat, sloping abruptly at the valve face/mantle junction, visible in LM as a darker circular edge. Spiraling to straight thick, siliceous ridges extending from the valve

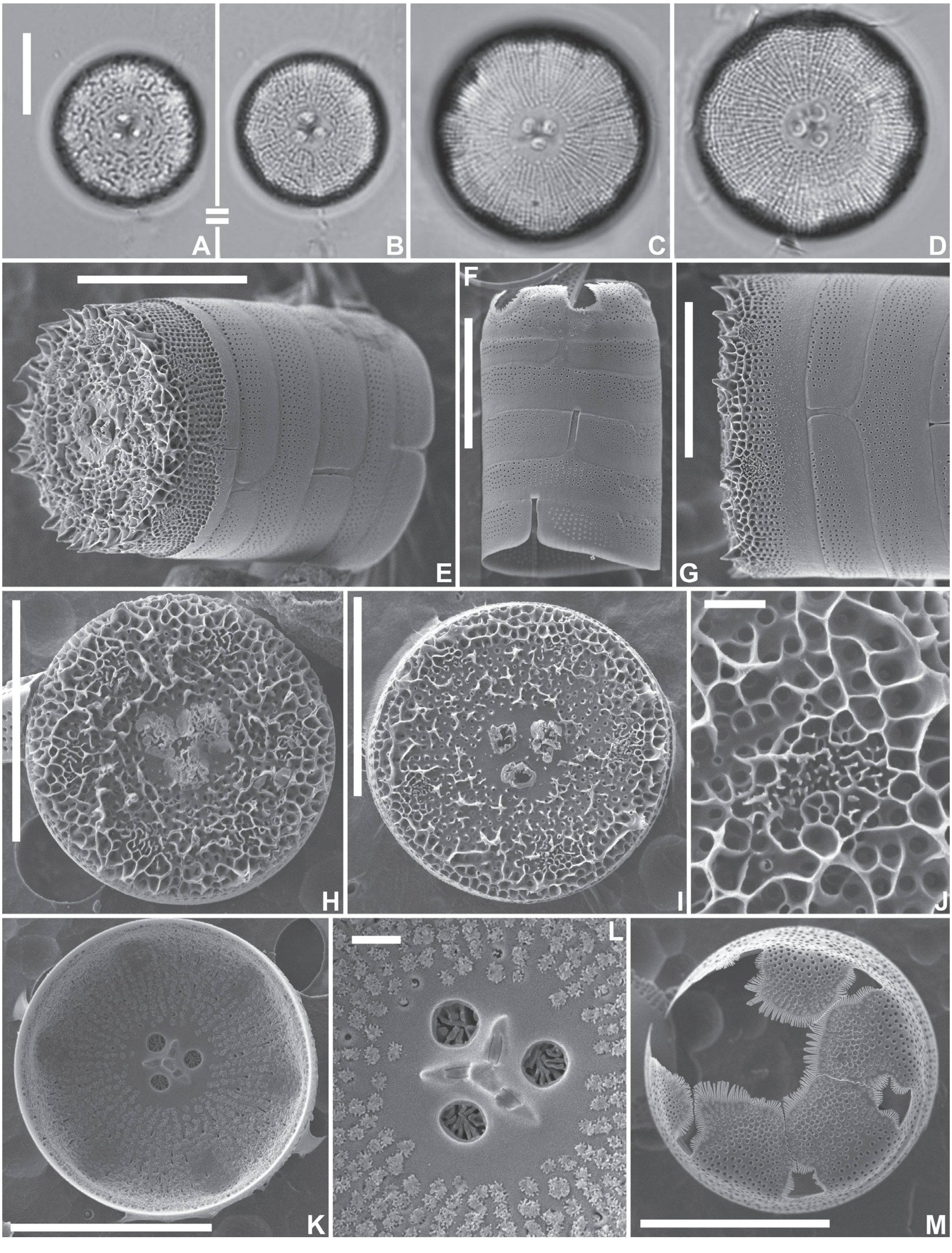

Figure 1. *Orthoseira hawaiiensis* Danz & Kociolek. LM (A–D) and SEM (E–M) micrographs taken from sample 110 (Karkar Island, Village of Mom, Papua New Guinea). **A**–**D**. LM pictures of valves in valve face view. **E**. SEM external view of a valve in oblique view showing the step in the mantle, the marginal ring of spines and the valve face ornamentation. **F**. Frustule in girdle view showing the structure of the cingulum. **G**. SEM detailed view of linking spines and mantle structure. **H**–**I**. SEM external view of a valve face. **J**. SEM external detail of denser grouping of short and longer ridges between areolae on the valve face. **K**. Internal view of a complete valve. **L**. SEM internal detail of the carinoportulae. **M**. External view of valvocopula. Scale bars: A–I, K, M = 10 μm; J, L = 2 μm.

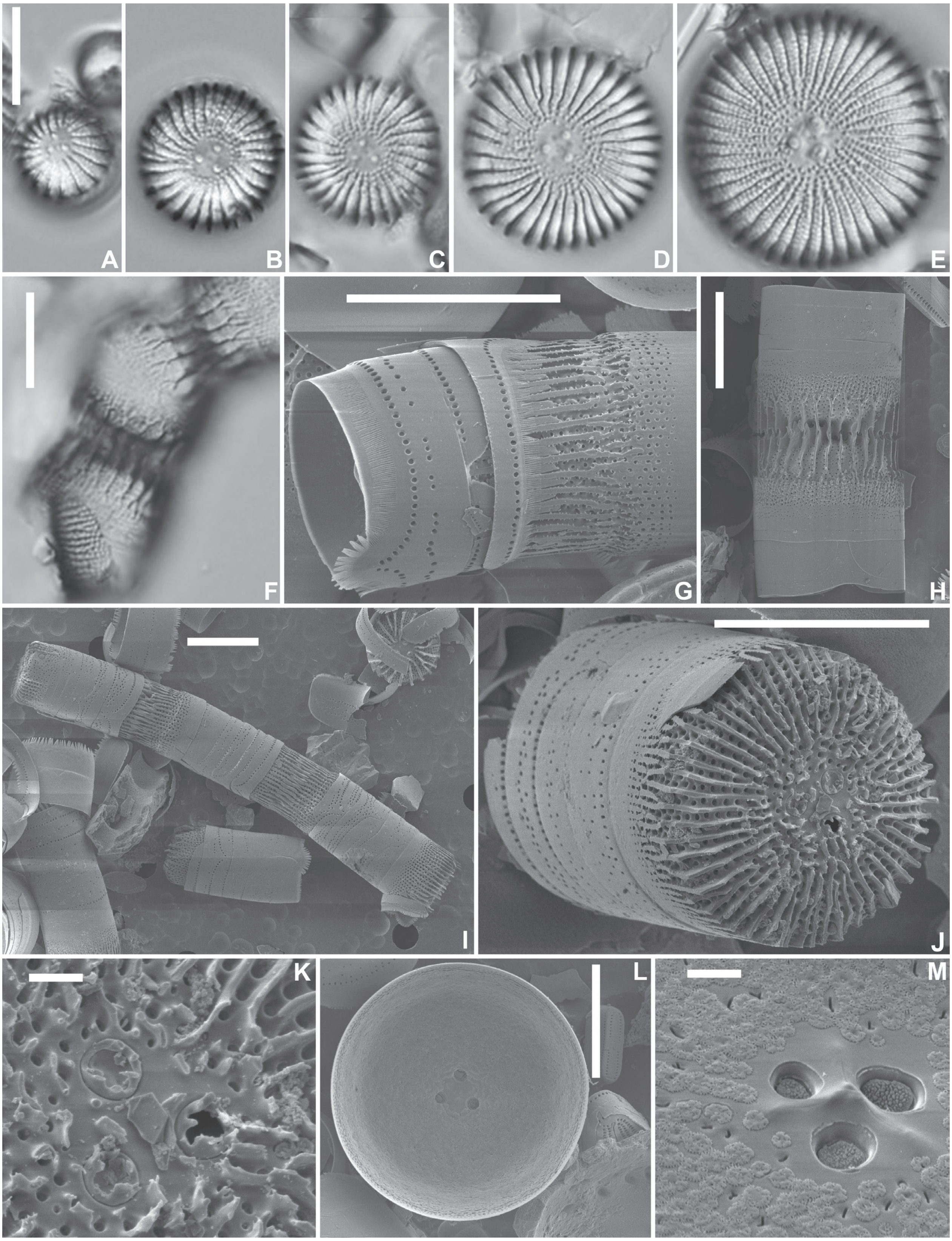

Figure 2. *Orthoseira tropica* (Krasske) Metzeltin & Lange-Bert. LM (A–E) and SEM (F–M) micrographs taken from sample 156 (Boisa Island, Papua New Guinea). **A**–**E**. LM pictures of valves in valve face view. **F**. Frustule in girdle view connected to each other with spines forming short chains. **G**–**I**. Frustule in girdle view showing the structure of the cingulum and linking spines. **J**. SEM external view of a valve in oblique view showing valve face structure. **K**. SEM external detail of central part of the valve face with carinoportulae. **L**. Internal view of a complete valve. **M**. SEM internal detail of the carinoportulae showing the slits between the carinoportulae, arranged in a star-shaped manner. Scale bars: A–J, L = 10 µm; K, M = 2 µm.

edge to almost 2/3 onto the valve face, leaving only a small central area. Central area small, maximum 1/4 to 1/5 of the total valve diameter, irregular in shape, hyaline in the middle, surrounded by short series of scattered areolae. Three large, rounded carinoportulae present, number constant irrespective of the valve diameter. Striae on the mantle short, uniseriate, composed of rather large areola, located between the ridges, 16–18 in 10 μm. Valve face areolae rather small, arranged in irregular uniseriate striae, ca 22 in 10 μm. Caverns, internal undulations or internal valves not observed. Copulae number variable. Figure 2A–F.

SEM description. Cingulum composed of several broad, open copulae. One complete and one incomplete rows of small poroids present on the copulae (Fig. 2 G–I). All copulae open bearing a long ligula and fimbriate edge (Fig. 2G–I). Mantle rarely shallow (Fig. 2J), usually deep (Fig. 2H), occasionally with a clear step halfway the valve mantle (Fig. 2H). Advalvar mantle edge with several irregular series of small areolae (Fig. 2G, J). Abvalvar edge broad, hyaline. Marginal pore fields absent. Platelike ridges extending from the valve face onto the advalvar edge of the mantle. Areolae visible between the ridges (Fig. 2G, H). Valve face flat in the central part surrounded by a ring of spiralling to straight, platelike linking structures, radially arranged on the valve face/mantle junction (Fig. 2J). Between the plates, up to three series of areolae present. Central area hyaline surrounded by scattered areolae. Three carinoportulae visible, each surrounded by a low, cylindrical collar (Fig. 2J–K). Areolae covered in the valve interior by individual hymenate vela (Fig. 2L, M). Carinoportulae pit-like, visible as large, rounded depressions, filled with siliceous plug (Fig. 2M). Between the carinoportulae, three long slits present (Fig. 2M), arranged in a star-shaped manner. Internal caverns not observed. Figure 2G–M.

Orthoseira iserentantii Kochman-Kędziora & Van de Vijver, **sp. nov.**

Fig. 3

Type locality. Mont Wilhelm, Papua New Guinea, 9 Apr. 1987, leg. M. Fagnant.

Type. Mont Wilhelm, Papua New Guinea, sample 17; holotype: slide BR-4817, BR; the valve representing the type is illustrated here in Fig. 3F; isotype: slide 433, University of Antwerp, Belgium.

Registration. http://phycobank.org/104292

LM description. Frustules cylindrical in girdle view. Valves disc-shaped. Valve dimensions (n = 20): diameter 8.0–21.5 μm, mantle height 5.0–7.5 μm. Valve face flat, sloping abruptly at the valve face/mantle junction, visible in LM as a darker circular edge. Central area very small, maximum 1/5 of the total valve diameter, irregular in shape. Three large, rounded carinoportulae present, number constant irrespective of the valve diameter. Between the carinoportulae scattered areolae present. Striae on the mantle long, uniseriate, ca 24 in 10 μm. Valve face areolae small, arranged in radiate, uniseriate striae, 20–22 in 10 μm. Caverns, internal undulations or internal valves not observed. Figure 3A–G.

SEM description. Cingulum composed of open, ligulate girdle bands bearing several, often incomplete, rows of large, rounded poroids (Fig. 3H–I). Parallel, uniseriate series of rounded, fairly large areolae present on the valve mantle, ca 24 in 10 μm. Often a clear step present halfway the valve mantle (Fig. 3J). Valve face flat, plate-like structures, irregular in shape, surrounding the entire valve face (Fig. 3K, L). Plate-like structures lacking perforations become linking plates, continuing onto the mantle as weakly raised, sometimes bifurcated ridges, flattening in the middle of the mantle height (Fig. 3H, J–L). Irregular pattern of smaller siliceous ridges, varied in length, present in the central part of the valve face, also between carinoportulae (Fig. 3L, N). Usually three carinoportulae surrounded by a siliceous collar present in very small pore-free central area (Fig. 3L, N). Striae radial composed of rounded areolae. Striae between ridges continuing on the mantle (Fig. 3H, K). Internally areolae appearing as small poroids with irregular caltrop-like structure inside (Fig. 3M, O, P). Slit-like openings present between the areolae (Fig. 3P). Carinoportulae unoccluded, ornamented with small granules (Fig. 3O). Between the carinoportulae, three long slits present (Fig. 3O), arranged in a star-shaped manner. Internal caverns not observed. Figure 3H–P.

Etymology. The species is named in honour of our (retired) colleague Dr Robert Iserentant (UCL, Belgium) to honour his life-long career as a diatom scientist.

Orthoseira papuensis Kochman-Kędziora & Van de Vijver, **sp. nov.**

Fig. 4

Type locality. Boisa Island, Papua New Guinea, sample 158, 4°00’00”S, 144°57’30”E, elev. 20 m a.s.l., 30 Dec. 1989, leg. R. Iserentant.

Type. Boisa Island, Papua New Guinea, sample 158; holotype: slide BR-4818, BR; the valve representing the type is illustrated here in Fig. 4F; isotype: slide 434, University of Antwerp, Belgium.

Registration. http://phycobank.org/104293

LM description. Frustules cylindrical in girdle view, connected to each other forming short chains (Fig. 4G, H). Valves disc-shaped. Valve dimensions (n = 20): valve diameter 6.5–23.0 μm, mantle height 8.0–9.5 μm. Valve face flat, sloping abruptly at the valve face/mantle junction, visible in LM as a darker circular edge. Central area small, maximum 1/4 of the total valve diameter, irregular in shape. Three to four large, rounded carinoportulae present. Between the carinoportulae scattered areolae present. Striae on the mantle long, uniseriate, 22–24 in 10 μm. Valve face areolae rather small, arranged in radiate, uniseriate striae, 16–22 in 10 μm. Caverns, internal undulations or internal valves not observed. Figure 4A–H.

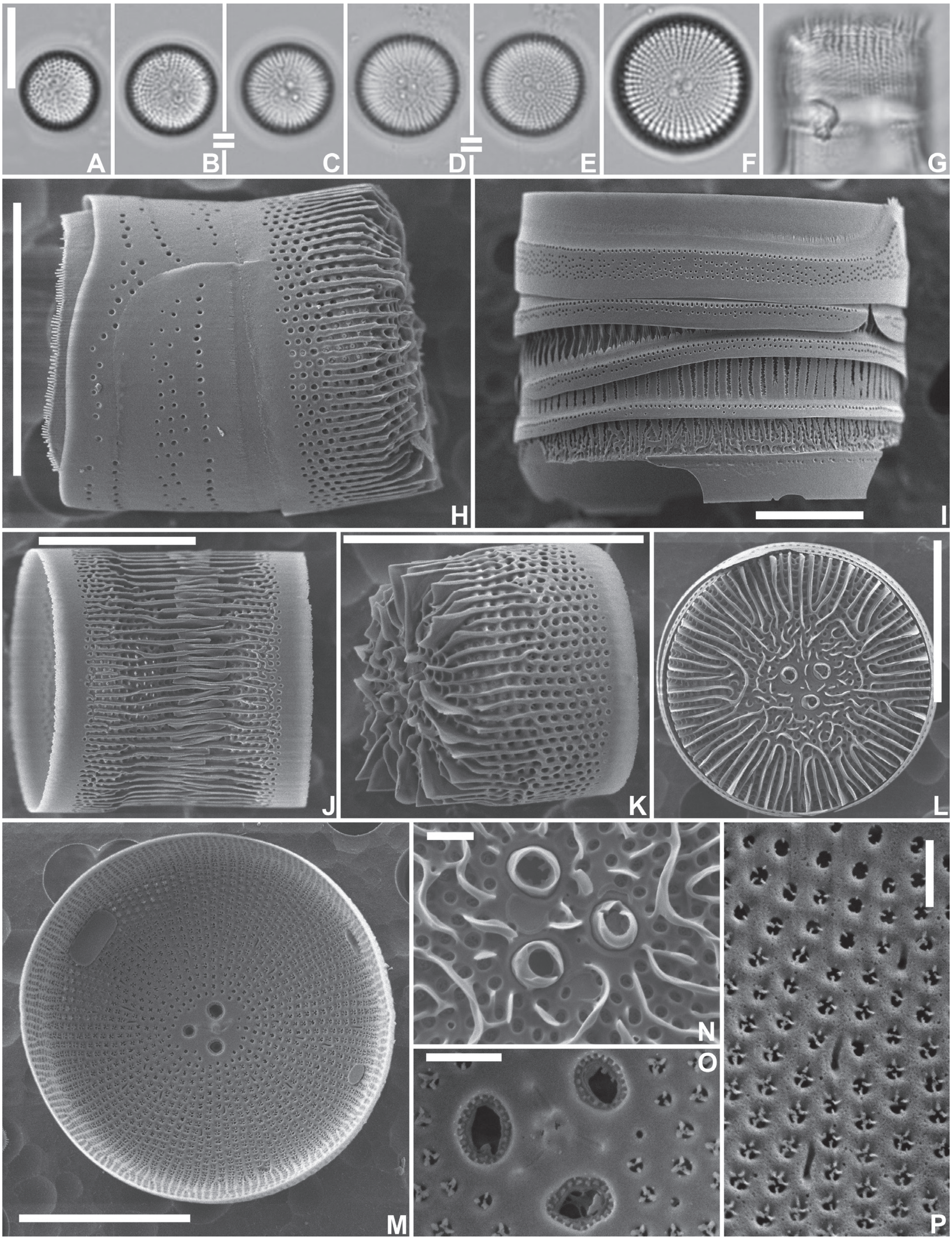

Figure 3. *Orthoseira iserentantii* Kochman-Kędziora & Van de Vijver sp. nov. LM (A–G) and SEM (H–P) pictures taken from the holotype material (BR-4817, sample 17, Mont Wilhelm, Papua New Guinea). **A**–**F**. LM pictures of valves in valve face view. **G**. Valve in girdle view showing marginal spines. **H**–**I**. SEM pictures of frustules in girdle view showing the structure of girdle bands. **J**. Sibling valves in girdle view showing the structure of linking plates. **K**. SEM external detail of linking plates and mantle structure. **L**. SEM external view of a valve face showing the structure of plates and smaller siliceous ridges. **M**. SEM internal view of a complete valve. **N**. SEM external detail of the central part of the valve face showing carinoportulae surrounded by a siliceous collar and the network of small siliceous ridges. **O**. SEM internal detail of the carinoportulae ornamented with small granules. **P**. SEM internal detail of the areolae and slit-like openings present between the areolae. Scale bars: A–M = 10 μm; N–P= 1 μm.

SEM description. Valve face flat, striae radial composed of round rimmed areolae (Fig. 4L). Near the valve edge, areolae slightly larger (Fig. 4I–K). Irregular pattern of small siliceous curving ridges, of variable length and shape, present over the entire valve face, including between the carinoportulae. Several (3–4) carinoportulae in the central area, surrounded by irregular siliceous circular ridges (Fig. 4J, L), often obscured by plate-like coverings (Fig. 4I, K). Small acute spines irregularly scattered along the valve face/mantle junction, occasionally absent (Fig. 4I, K, M). Mantle very deep composed of two parts, advalvar with areolae organised in parallel, uniseriate series, 22–24 in 10 µm, located between weakly raised ridges. Ridges flattering in the middle of the mantle, followed by a hyaline, non-perforated abvalvar part (Fig. 4M, O). Internally areolae occluded with individually hymenate vela (Fig. 4N). Carinoportulae pit-like, formed by large rounded foramina, filled with siliceous plug (Fig. 4N). Between the carinoportulae, three long slits present (Fig. 4N), arranged in a star-shaped manner. Internal caverns not observed. Cingulum composed of broad, open, ligulate girdle bands, perforated with a large number of scattered poroids, irregularly organised in parallel series (Fig. 4M, O). Figure 4I–O.

Etymology. The specific epithet "*papuensis*" refers to the geographic locality where the new species was found.

Ecology and associated diatom species

All samples used in this study were collected from terrestrial mosses with a varying degree of moisture content. Sample 17 was taken from wet *Hypnum* mosses on trunks of several Ericaceae bushes. Water squeezed out of the mosses had a pH of 5.4. The sample, used for the description of *O. iserentantii*, is dominated by several *Eunotia* species with the most abundant one showing a high similarity to *E. sphagnicola* Van de Vijver, A.Mertens & Lange-Bert., *Stauroneis obtusa* Lagerst., and *Humidophila* cf. *potapovae* R.L.Lowe, Kociolek & Q.You. This diatom flora, although rather species-poor, is commonly found in wet acidic terrestrial mosses. The second sample in this study, sample 110, was collected on Karkar Island, a small (total area 360 km^2) island in the Bismarck Sea, close to the coast of Papua New Guinea. The diatom composition in the sample is rather species poor and contains almost exclusively species from the genera *Humidophila* (mainly *H. paracontenta* var. *magisconcava* (Lange-Bert.) R.L.Lowe, Kociolek, J.R.Johans., Van de Vijver, Lange-Bert. & Kopalová), *Luticola* (*L.* cf. *isabellae* Metzeltin & Levkov and *L. acidoclinata* Lange-Bert.), *Pinnularia* (mainly an unknown species from the *P. borealis* Ehrenb. group), and *Hantzschia* (such as *H. amphioxys* (Ehrenb.) Grunow in Cleve and Grunow 1880). These genera are very typical in dry to moist, terrestrial (= aerophytic) environments (Lange-Bertalot et al. 2017). Samples 156 and 158 were collected on a second Papuan island, Boisa Island, a very small (total area 1.29 km^2), flattened volcanic islet located not far from Karkar Island. Both samples contain large populations of several *Humidophila* species (*H. paracontenta* var. *magisconcava* in sample 156, *H.* cf. *potapovae* in sample 158), *Luticola* (mainly *L. acidoclinata* but also *L. hustedtii* Levkov, Metzeltin & A.Pavlov), *Hantzschia* cf. *amphioxys*, and *Pinnularia* (*borealis*-group). Sample 156 is dominated by *Orthoseira tropica*, whereas sample 158 is characterised by a larger population of *O. papuensis*. Given the subtle difference in sample description between both samples (156 from slightly wet mosses, 158 from rather dry mosses), this may indicate that *O. tropica* prefers wetter (or at least more moist) conditions and *O. papuensis* is mainly found in drier circumstances. More samples will have to be analysed to determine the exact ecological preferences of each species.

DISCUSSION

The morphology of all four species corresponds to the description of the genus *Orthoseira* as defined by Crawford (1981), based on the presence of the typical carinoportulae, the broad perforated copulae and the deep mantle. The four species each present a unique combination of features allowing the ability to separate them in both LM and SEM. Differences between the four species include the presence of internal caverns visible on the valve interior as marginal porefields (*O. hawaiiensis*), the presence of small slits between the areolae in the valve interior (*O. hawaiiensis*, *O. tropica*, and *O. iserentantii*), the number of rows of perforations on the copulae (maximum 2 in *O. tropica*, multiple in the other three), the presence of plate-like linking structures (*O. tropica* and *O. iserentantii*), the presence of marginal spines (*O. hawaiiensis* and *O. papuensis*), and the external structure of the carinoportulae (with plate-like coverings in *O. hawaiiensis* and *O. papuensis*, open in *O. tropica* and *O. iserentantii*). Whether these differences will allow the separation of groups within *Orthoseira* sensu Crawford (1981) can only be confirmed after a thorough cladistic analysis, which is out of the scope of the present paper.

Two species were previously described from Hawaii (*O. hawaiiensis*, Danz and Kociolek 2022) and South America (*O. tropica*, Krasske 1948).

Orthoseira hawaiiensis has up to now only been observed on Maui Island (Hawaii, Danz and Kociolek 2022). Comparison between the type population and Papua New Guinea population in the present paper, revealed no clear morphological differences, apart from the observation of some specimens with only two carinoportulae (whereas Danz and Kociolek (2022) strictly mention 3 carinoportulae). Both populations have externally covered carinoportulae, areas on the valve face with denser ridge aggregations, organised in a circular pattern, short, robust marginal spines, internal caverns, multiareolate broad copulae, and internal slits between the carinoportulae, justifying the proposed conspecificity (Danz and Kociolek 2022). The maximum

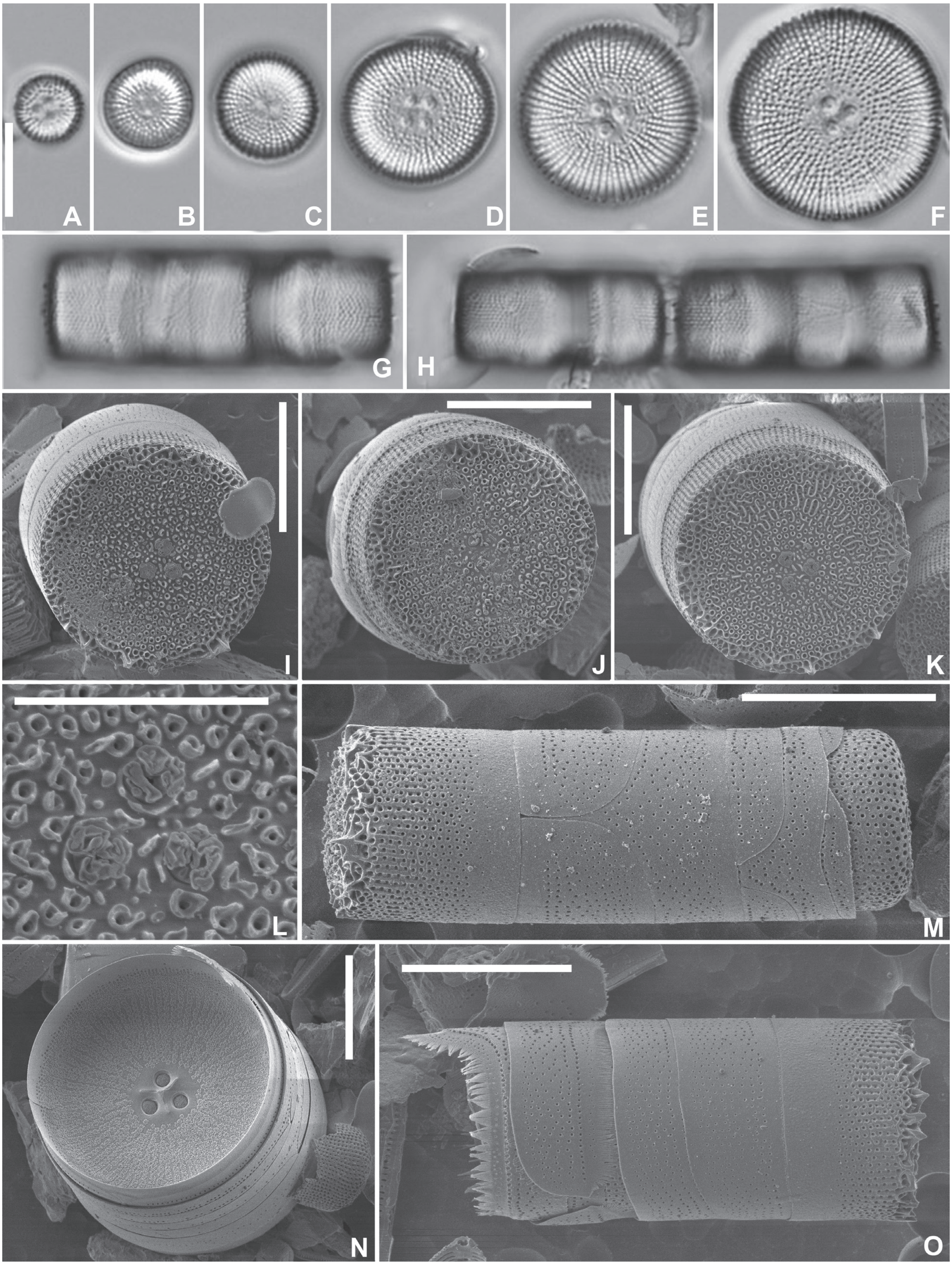

Figure 4. *Orthoseira papuensis* Kochman-Kędziora & Van de Vijver sp. nov. LM (A–H) and SEM (I–O) pictures taken from the holotype material (BR-4818, sample 158, Boisa Island, Papua New Guinea). **A**–**F**. LM pictures of valves in valve face view. **G**–**H**. Frustules in girdle view. **I**–**K**. SEM external view of a valve face. **L**. SEM external detail of central part of the valve face with carinoportulae. **M**, **O**. Valves in girdle view with perforated girdle bands. **N**. Internal view of a complete valve. Scale bars: A–K, M–O = 10 μm; L = 5 μm.

valve diameter in Danz and Kociolek (2022) is more than double that of the observed diameter in the Papua New Guinea population. However, as the diameter range of the Papua New Guinea population is entirely fitting within the Hawaiian range, this difference should be neglected. Interestingly, *O. hawaiiensis* was described from mosses growing in lava tubes, whereas the Papua New Guinea population was found on moist liverworts growing on a tree trunk.

Lange-Bertalot et al. (1996) illustrated *Melosira roeseana* var. *tropica* Krasske with two (partial) LM images (Lange-Bertalot et al. 1996: plate 53, figs 5, 6). At present, this is the only representation of the type population of this species that is currently available. Rybak et al. (2022) observed and illustrated a large population of *O. tropica* on Palambak Island (Indonesia). Based on its morphology, the Papua New Guinea population in the present paper shows a large similarity with the Palambak population, but also presents several morphological differences. Similarities include the often spiralling plate-like structures, the broad girdle bands with maximum 2 rows of perforations, and the siliceous outgrows on the plate-like structures (see Fig. 2G). In the Palambak population, at least 2, but more often 3–4 rows of areolae are present between the plate-like linking spines similar to the Papua New Guinea population, where also 1–4 rows of areolae can be seen (Rybak et al. 2022: figs 34–36, and our Fig. 2H, J). On the other hand, the hyaline central area in the Palambak population is much larger than the central area in the Papua New Guinea population; in the latter, the areolae is almost touching the carinoportulae (see Rybak et al. 2022: figs 34–36 compared with our Fig. 2J, K). Whether the latter difference is sufficient to separate both populations is unclear: firstly, a better knowledge of the morphological variability of the type of *O. tropica* is necessary; and secondly, more populations identified as *O. tropica* should be analysed, to verify how variable this feature is.

The two other species are described as new, as they present clear differences with all known species. *Orthoseira iserentantii* shows a high degree of similarity with *Orthoseira radiata* M.Rybak, Glushchenko & Kulikovskiy, described from Palambak Island in Indonesia (Rybak et al. 2022). However, analysis of the valves illustrated in Rybak et al. (2022: figs 101–106) shows that most likely fig. 102, taken from a specimen from Rapa Nui (Easter Island), illustrates a valve that does not belong to *O. radiata*, based on significant differences in mantle striae, hyaline central area and the siliceous ridges on the valve face. Both *O. iserentantii* and *O. radiata* have overlapping valve dimensions, although *O. iserentantii* has a slightly higher mantle areola density (ca 24 vs 20–22 in *O. radiata*). The two species differ in the arrangement of the raised siliceous ridges on the valve mantle, the structure of the copulae, the striation pattern on the mantle and the internal valve view. *Orthoseira iserentantii* presents an irregular network of raised siliceous ridges in the central area, even between the carinoportulae. Part of these ridges is connected to the plate-like linking structures. Similar structures can also be found in *Orthoseira radiata*, although in this species the ridges are shorter and more irregularly shaped ridges (Rybak et al. 2022: figs 101, 104). Additionally, the mantle in *O. iserentantii*, besides having a higher areola density, is composed of areolae with a cribrate internal structure that is even visible in the external view. In *O. radiata*, this cribrate structure does not seem to be present, based on Rybak et al. (2022: fig. 105). The copulae in *O. radiata* appear to be very broad, bearing multiple rows of small areolae, whereas in *O. iserentantii* the copulae are narrower with only two or a few rows of large areolae. Finally, both species can be separated based on their internal structure. The areolae in *O. radiata* are occluded by a velum, whereas in *O. iserentantii* they have a cribrate structure (although it is possible that the vela have been eroded, even though this was not the case in the other *Orthoseira* species analysed in this study that have been prepared simultaneously in the same way). Additional features such as the slit-like openings between striae and the delicate ornamentation of the carinoportulae in *O. iserentantii*, are absent in *O. radiata*. Given that Rybak et al. (2022: fig. 102) probably does not belong to *O. radiata* and based on the statement that *O. radiata* is characterized by a high morphological variability (Mateusz Rybak pers. comm.), it is possible that fig. 102 represents *O. iserentantii*, indicating that the samples analysed by Rybak et al. (2022) most likely contain more species, including *O. iserentantii*, than actually reported. Further analysis of the Palambak and Rapa Nui samples in Rybak et al. (2022) will be necessary to confirm the species identity of the specimens presented by Rybak et al. (2022: fig. 102).

Orthoseira papuensis sp. nov. can be confused with *O. cylindrica* M.Rybak, Glushchenko & Kulikovskiy (Rybak et al. 2022), especially when using only light microscopy observations. Both species overlap in valve diameter (5.8–26.0 µm in *O. cylindrica* vs 8.0–21.5 in *O. papuensis*), but have a different stria density (22–24 in *O. cylindrica* vs 16–22 in *O. papuensis*). The ultrastructure of both species, as revealed by the SEM analysis shows that both species are quite distinct. The valve face of *O. cylindrica* is ornamented with radiating striae composed of round, rimmed areolae (Rybak et al. 2022: figs 49, 50, 52), contrarily to *O. papuensis*, in which the valve surface is characterised by a combination of rimmed areolae and an irregular pattern of small, irregularly long siliceous ridges that are present on the entire valve face, including between carinoportulae. Similar ridges are almost absent in *O. cylindrica*. Both species also differ in the arrangement of the pores on the girdle bands. Whereas on the girdle bands of *O. cylindrica* the pores are organised in rows (Rybak et al. 2022: fig. 54), the girdle bands in *O. papuensis* have a less organised pattern of pores (see Fig. 4M). Internally, *O. cylindrica* has areolae covered by well separated individual vela (Rybak et al. 2022: fig. 51), whereas in *O. papuensis*, the areolae are covered by an apparently continuous strip of fused vela running from valve margin to the carinoportulae (Fig. 4N).

CONCLUSIONS

The discovery of two new *Orthoseira* species on Papua New Guinea shows that there is still a large unknown aerophilic diatom flora present in remote places on Earth. Nevertheless, the observation of two other, previously described tropical *Orthoseira* species proves that there might be a pool of tropical aerophilic species present in environmentally similar habitats worldwide. The results also showed that due to lumping and force-fitting, the actual diversity of the genus *Orthoseira* is still poorly understood. Unpublished results from the sub-Antarctic regions showed that the reported, presumable cosmopolitan species in that region, in fact have to be described as new species, showing distinct differences with for instance *O. roeseana* s.s. A better understanding of the morphology of the different *Orthoseira* populations worldwide will most likely result in a better delimitation of all *Orthoseira* species, confirming the growing idea that even in aerophilic, seemingly cosmopolitan species, a distinct bioregionalisation is far more realistic.

ACKNOWLEDGEMENTS

The research done by Natalia Kochman-Kędziora received support from the SYNTHESYS project (www.synthesys.info), which is financed by the H2020 Research Infrastructures Programme, to visit Meise Botanic Garden. Prof. Robert Iserentant and Mrs Martine Fagnant are thanked for collecting the samples in 1987 and 1989.

REFERENCES

Cleve PT, Grunow A (1880) Beiträge zur Kenntniss der Arktischen Diatomeen. Kongliga Svenska-Vetenskaps Akademiens Handlingar 17(2): 1–121.

Crawford RM (1981) The diatom genus *Aulacoseira* Thwaites: its structure and taxonomy. Phycologia 20: 174–192. https://doi.org/10.2216/i0031-8884-20-2-174.1

Danz A, Kociolek JP (2022) Four new *Orthoseira* Thwaites species from Maui, Hawaii, and the Columbia River Gorge, Oregon, with comments on frustular morphology in the genus. Diatom Research 37: 17–37. https://doi.org/10.1080/0269249X.2022.2044911

Danz A, Van de Vijver B, Kochman-Kędziora N, Kusber WH, Guerrero J, Vouilloud A, Sala SE, Liu Q, Kociolek JP (2022) The genus *Orthoseira* Thwaites: historical overview, current status and recommendations for the future. Nova Hedwigia 115: 1–29. https://doi.org/10.1127/nova_hedwigia/2022/0692

Ehrenberg CG (1848) Über eigenthümliche auf den Bäumen des Urwaldes in Süd-Amerika zahlreich lebende mikroskopische oft kieselschalige Organismen. Bericht über die zur Bekanntmachung geeigneten Verhandlungen der Königlich-Preussischen Akademie der Wissenschaften zu Berlin 1848: 213–220.

Gargas CB, Theriot EC, Ashworth MP, Johansen JR (2018) Phylogenetic analysis reveals that the 'radial centric' diatom *Orthoseira* Thwaites (Orthoseiraceae, Bacillariophyta) is a member of a 'multipolar' diatom lineage. Protist 169: 803–825. https://doi.org/10.1016/j.protis.2018.08.005

Goeyers C, Kochman-Kędziora N, Van de Vijver B (2023) *Orthoseira groenlandica* sp. nov., a new aerophilic diatom (Orthoseirales, Bacillariophyta) species from Greenland. Phytotaxa 601(1): 81–89. https://doi.org/10.11646/phytotaxa.601.1.6

Guerrero JM, Vouilloud AA, Sala SE, Kociolek JP, Van de Vijver B (2018) New species and a new genus of the Orthoseirales from Patagonia, Argentina, with comments on systematic affinities within the order. Phytotaxa 345(2): 119–132. https://doi.org/10.11646/phytotaxa.345.2.3

Guiry MD, Guiry GM (2023) AlgaeBase.World-wide electronic publication, National University of Ireland, Galway. https://www.algaebase.org [accessed 21.10.2023]

Houk V (1993) Some morphotypes in the "*Orthoseira roeseana*" complex. Diatom Research 8: 385–402. https://doi.org/10.1080/0269249X.1993.9705269

Houk V, Klee R, Tanaka H (2017) Atlas of freshwater centric diatoms with a brief key and descriptions. Second emended edition of part I and II. Melosiraceae, Liparogyraceae, Paraliaceae and Aulacoseiraceae. Fottea 17(Supplement): 1–616.

Kochman-Kędziora N, Kusber WH, Kociolek JP, Van de Vijver B (2023) Observations on the type material of *Melosira roeseana* Rabenhorst and W.Smith (Orthoseiraceae, Bacillariophyta). Notulae Algarum 274: 1–10.

Kociolek JP, Liu Q, Danz A (2021) New and interesting diatoms from the Shimen Wetwalls, Yunnan province, China. I. Valve morphology of *Melosira radiato-sinuata* var. *yunnanica* Chen (Bacillariophyta: Melosirales) from Yunnan province, China, with comments on its systematic position. Diatom Research 36: 345–351. https://doi.org/10.1080/0269249X.2021.2025151

Krasske G (1948) Diatomeen tropischer Moosrasen. Svensk Botanisk Tidskrift 42(4): 404–443.

Kützing FT (1844) Die Kieselschaligen Bacillarien oder Diatomeen. W. Köhne, Nordhausen, 1–152. https://doi.org/10.5962/bhl.title.64360

Lange-Bertalot H, Külbs K, Lauser T, Nörpel-Schempp M, Willmann M (1996) Dokumentation und Revision der von George Krasske beschriebenen Diatomeen-Taxa. Iconographia Diatomologica 3: 1–358.

Lange-Bertalot H, Hofmann G, Werum M, Cantonati M (2017) Freshwater Benthic Diatoms of Central Europe. Koeltz Botanical Books, Schmitten-Oberreifenberg, 1–942.

Lowe RL, Kociolek JP, Van de Vijver B (2013) Two new *Orthoseira* species (Bacillariophyceae) from lava tubes on Ile Amsterdam and Big Island (Hawai'i). Phytotaxa 111: 39–52. https://doi.org/10.11646/phytotaxa.111.1.3

Metzeltin D, Lange-Bertalot H (2007) Tropical diatoms of South America II. Special remarks on biogeography disjunction. Iconographia Diatomologica 18: 1–877.

Peszek Ł, Robinson CT, Rybak M, Kawecka B (2023) *Orthoseira helvetica* sp. nov. – a new diatom (Bacillariophyceae) from the Swiss Alps. Diatom Research 38(2):77–87. https://doi.org/10.1080/0269249X.2023.2230972

Pfitzer E (1871) Untersuchungen über Bau und Entwicklung der Bacillariaceen (Diatomaceen). Botanische Abhandlungen aus dem Gebiet der Morphologie und Physiologie 2: 1–189.

Rabenhorst L (1853) Die Süsswasser-Diatomaceen (Bacillarien.): für Freunde der Mikroskopie. Eduard Kummer, Leipzig, 1–72, 10 pls.

Ross R, Cox EJ, Karayeva NI, Mann DG, Paddock TBB, Simonsen R, Sims PA (1979) An amended terminology for the siliceous components of the diatom cell. Nova Hedwigia, Beiheft 64: 513–533.

Round FE, Crawford RM, Mann DG (1990) The Diatoms. Biology and Morphology of the Genera. Cambridge University Press, New York, 1–747.

Rybak M, Glushchenko A, Witkowski A, Lange-Bertalot H, Kulikovskiy M (2022) Diversity of the genus *Orthoseira* Thwaites (Bacillariophyceae) from Southeast Asia and Rapa Nui Island with descriptions of four new taxa. Diatom Research 37: 1–16. https://doi.org/10.1080/0269249X.2022.2043448

Smith W (1855) Notes of an excursion to the south of France and the Auvergne in search of Diatomaceae. Annals and Magazine of Natural History, Series 2 15: 1–9.

Thwaites GHK (1848) Further observations on the Diatomaceae with descriptions of new genera and species. Annals and Magazine of Natural History, Series 2 1: 161–172.

Turland NJ, Wiersema JH, Barrie FR, Greuter W, Hawksworth DL, Herendeen PS, Knapp S, Kusber W-H, Li D-Z, Marhold K, May TW, McNeill J, Monro AM, Prado J, Price MJ, Smith GF (2018) International Code of Nomenclature for Algae, Fungi, and Plants (Shenzhen Code) Adopted by the Nineteenth International Botanical Congress Shenzhen, China, July 2017. Regnum Vegetabile 159. Glashütten, Koeltz Botanical Books, 1–253. https://doi.org/10.12705/Code.2018

Van de Vijver B, Kopalová K (2008) *Orthoseira gremmenii* sp. nov., a new aerophilic diatom from Gough Island (southern Atlantic Ocean). Cryptogamie, Algologie 29: 105–118.

Van de Vijver B, Beyens L, Vincke S, Gremmen NJ (2004) Moss-inhabiting diatom communities from Heard Island, sub-Antarctic. Polar Biology 27: 532–543. https://doi.org/10.1007/s00300-004-0629-x

van der Werff A (1955) A new method of concentrating and cleaning diatoms and other organisms. Verhandlungen der internationalen Vereinigung für theoretische und Angewandte Limnologie 12(1): 276–277. https://doi.org/10.1080/03680770.1950.11895297